Applied Physics Letters

Chemical bonding and band alignment at X_2O_3/GaN (X = Al, Sc) interfaces

Cite as: Appl. Phys. Lett. **114**, 161601 (2019); https://doi.org/10.1063/1.5097567
Submitted: 26 March 2019 . Accepted: 12 April 2019 . Published Online: 26 April 2019

Zhaofu Zhang, Yuzheng Guo, and John Robertson

Applied Physics Letters ARTICLE scitation.org/journal/apl

Chemical bonding and band alignment at X_2O_3/GaN (X = Al, Sc) interfaces

Cite as: Appl. Phys. Lett. **114**, 161601 (2019); doi: 10.1063/1.5097567
Submitted: 26 March 2019 · Accepted: 12 April 2019 ·
Published Online: 26 April 2019

Zhaofu Zhang,[1] Yuzheng Guo,[2] and John Robertson[1,a)]

AFFILIATIONS

[1]Department of Engineering, Cambridge University, Cambridge CB2 1PZ, United Kingdom
[2]College of Engineering, Swansea University, Swansea SA1 8EN, United Kingdom

[a)]Author to whom correspondence should be addressed: jr214@cam.ac.uk.

ABSTRACT

The chemical bonding and the band alignment at Al_2O_3/GaN and Sc_2O_3/GaN interfaces are studied using density functional supercell calculations. Using bonding models based on the electron counting rule, we have created the insulating interfaces with a small roughness and a clean bandgap. Ga-O bonds dominate the interfacial chemical bonding at both interfaces. The calculated band alignment agrees with the experimental values. For the Al_2O_3 interface, the calculated valence band offset is 1.17 eV using hybrid functionals, while that for the Sc_2O_3 interface is 0.81 eV. The conduction band offsets for both are larger than 1 eV, and is as large as ∼2 eV for the Al_2O_3 interface. The calculated band alignments indicate that Al_2O_3 and Sc_2O_3 are both suitable insulators for GaN-based MOSFET applications.

Wide bandgap semiconductor GaN-based metal-oxide-semiconductor field effect transistors (MOSFETs) are promising candidates for next-generation high-voltage power devices beyond silicon.[1,2] Nevertheless, large concentrations of surface and/or interface states have hindered the device performance, leading to leakage currents and current collapse.[3] To supplement the flexibility of the device design to the maximum and enable novel functionalities in GaN-based electronics, the gate dielectric should be prudently selected. Sc_2O_3 with large bandgap (∼6 eV), high dielectric constant ($\varepsilon = 14$), and large band offset (BO) has been reported to deliver a low density of interface states (D_{it}) of $\sim 10^{12}\,eV^{-1}\,cm^{-2}$ with little leakage current at the Sc_2O_3/GaN interface in the past decade.[4,5] Later, the industrially preferred oxide Al_2O_3 became popular by virtue of high breakdown electric field (∼10 MV/cm), high thermal stability, favorable band alignment with GaN, as well as easier preparation by atomic-layer deposition (ALD) technique,[6–9] and the device performance has been dramatically improved.[10,11] Thus, both Sc_2O_3 and Al_2O_3 are suitable insulator materials for GaN-based MOSFET devices.

The interfaces of both oxide dielectrics on GaN have been extensively studied experimentally. The band offset, especially the conduction band offset (CBO), should be sufficiently large (>1 eV) to inhibit the Schottky emission of carriers and suppress the leakage current for a high-quality oxide/GaN interface.[12,13] In power devices, a larger CBO is more desirable considering the high-voltage gate driver requirement. Some previous work has reported the experimental BO values between GaN and oxide by x-ray photoemission spectroscopy (XPS), while the reported valence band offsets (VBOs) have a wide range of values from 0.05 eV to 2.1 eV for the Al_2O_3 interface,[6–9,14] and 0.4–0.8 eV for the Sc_2O_3 interface.[15,16] The large uncertainty brings trouble for fully understanding the quality of gate oxide. Furthermore, the microscopic understanding of the oxide/GaN interface properties is hindered by a lack of theoretical work on the detailed chemical bonding and band alignment of reasonable Al_2O_3/GaN and Sc_2O_3/GaN configurations. The accurate BOs should be attained based on the stable and insulating interface, where there are no gap states within the bandgap and the Fermi level lies at the midgap. To achieve this goal, the electron counting rule (ECR) must always be obeyed while constructing the interface.[17–19] Currently, there are only two calculations of the Al_2O_3/GaN interfaces, but these used the α-Al_2O_3 phase which has too large a band gap (∼8.8 eV), and the importance of electron-counting was ignored.[20,21]

In this work, the geometry and electronic properties of the interface between GaN and two trivalent oxides X_2O_3 (X = Al, Sc) are investigated in detail by first-principles calculations. To derive the band line-up with GaN, we first constructed X_2O_3/GaN interface models for a less ionic oxide Al_2O_3 and a more ionic oxide Sc_2O_3. The band offsets are then derived using the core-level method in the insulating interfaces.[22] Our results validate VBOs of 1.17 eV and 0.8 eV for Al_2O_3/GaN and Sc_2O_3/GaN, respectively, both within the range of measured values.

The calculations were carried out using the density functional theory (DFT) plane-wave CASTEP code.[23,24] A norm-conserving pseudopotential with a plane-wave cutoff energy of 700 eV was used for all calculations. Geometry relaxations were conducted using the Perdew-Burke-Ernzerhof version generalized gradient approximation (GGA-PBE) exchange-correlation functional[25] with a convergence criterion of 0.02 eV/Å for the force acting on each atom. A $5 \times 5 \times 1$ k-mesh was adopted. The electronic structures were evaluated using the Heyd-Scuseria-Ernzerhof (HSE) hybrid functional[26] to overcome the bandgap underestimation in the semilocal exchange-correlation functional. The Hartree-Fock exchange factor is tested to be 27%, yielding the direct bandgap of 3.4 eV for the wurtzite GaN bulk,[27,28] agreeing well with the experimental characteristics. Note that the calculated bandgaps for Al_2O_3 and Sc_2O_3 are 6.36 eV and 5.25 eV using this hybrid HF fraction, respectively, which are still 0.2 eV and 0.7 eV lower than the experimental values. The calculated total densities of states (DOSs) of the final relaxed bulk materials (structures shown in Fig. 1) are depicted in Fig. 2.

Although the deposited oxide normally adopts the amorphous phase, the essential requirement is the interface local bonding rather than the long-range crystalline symmetry to meet the valence satisfaction. Al_2O_3 possesses several symmetric phases, among which the most stable one is the hexagonal α-Al_2O_3 phase (i.e., corundum, or sapphire).[29] In the previous reports on Al_2O_3/GaN, α-Al_2O_3 was adopted, benefiting from a smaller lattice mismatch with wurtzite GaN.[20,21] However, the mass density (~4.0 g/cm^3) and the bandgap (~8.8 eV) of α-Al_2O_3 are too high compared to the amorphous one. Therefore, we adopted a modified θ-phase Al_2O_3 structure which has the mass density (~3.5 g/cm^3), the bandgap (~6.6 eV), and the atomic coordination close to the amorphous structure grown by ALD.[29,30] Al_2O_3 was strained to an orthorhombic structure and stretched laterally to achieve a good match with GaN (0001), before being fully relaxed to remove the stress. The atomic structure is shown in Fig. 1(b). For Sc_2O_3, the hexagonal phase was used [Fig. 1(c)], which matches GaN (0001) with a negligible lattice mismatch of only 3.7%. For the interface model, a thick vacuum (15 Å thickness) was added above the oxide to avoid the image interaction due to the periodic boundary condition, and the bottom N dangling bonds (DBs) in GaN were passivated by pseudo-hydrogens. Half of the top O atoms were removed to generate an insulating oxide surface without gap states.

It is noted that to create a closed-shell structure, we built the interface supercell model of (2×4) in-plane periodicity, which contains an oxide surface slab and a GaN (0001) slab with Ga-O bonding at the interface. The interface with Ga-O bonding is more stable than the one with X-Ga or X-N interfacial bonding, because Ga is trivalent like Al to make sure that the bonding characteristics of interfacial atoms are close to those in bulk materials. Besides, Chokawa *et al.* have reported that the Ga-Al interface shows much more interfacial defect states than the Ga-O model.[21] In this (2×4) interface, eight Ga and eight O atoms initially lie at the interface. For the covalent oxide Al_2O_3, the interfacial oxygen atoms perfectly saturate the Ga DBs. While for the ionic oxide Sc_2O_3, the structure is more complicated because both fourfold and sixfold O atoms exist in different layers within hexagonal Sc_2O_3. To gain the extra six electrons provided by eight Ga DBs, only four fourfold interfacial O atoms are required so that all the O DBs are occupied. Thus, we built the Sc_2O_3/GaN interface with only 50% interface O content (four fourfold interfacial O atoms) to satisfy the electron counting.

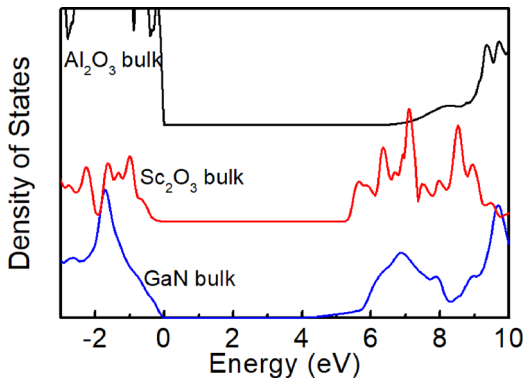

FIG. 2. Total densities of states of bulk Al_2O_3, Sc_2O_3, and GaN using the hybrid functional calculation. Note that the conduction band minimum (CBM) of GaN bulk is too weak and the bandgap is obtained from the gamma point data.

The lattice constant of relaxed GaN and Sc_2O_3 bulk is 3.24 Å and 3.36 Å, respectively. Since the Al_2O_3 structure was stretched laterally, it perfectly matches the GaN (0001) surface. As shown in the final Al_2O_3/GaN interface structures in Fig. 3(a), the atomic structure on the Al_2O_3 side becomes different from that in the crystalline phase, but the local bonding and the atomic coordinate remain the same. The interface is stable with a negligible roughness of only 0.3 Å at the interfacial Ga atom layer. The interfacial O atoms are either twofold or threefold, same as their bulk bonding characteristics. Eight Ga-O bonds form at the interface and each Ga atom occupies one Ga-O

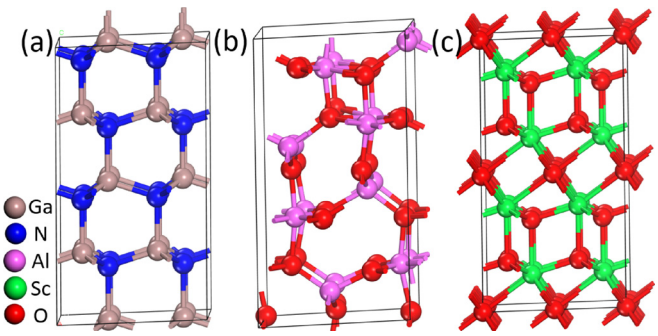

FIG. 1. The final relaxed structures of (a) GaN, (b) Al_2O_3, and (c) Sc_2O_3 bulk, respectively. The species of atoms are indicated in the inset.

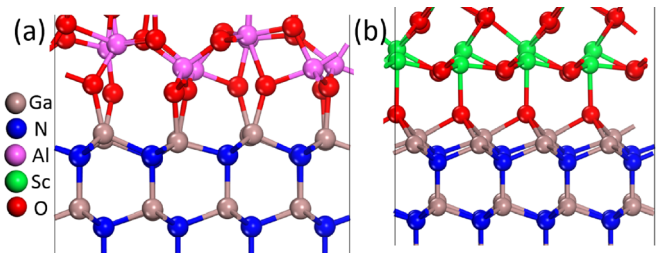

FIG. 3. The atomic structures of final relaxed (a) Al_2O_3/GaN and (b) Sc_2O_3/GaN interfaces. The species of atoms are indicated in the inset.

bond. This perfectly saturates the Ga DBs and leads to an insulating interface. The average interfacial Ga-O bond length is 1.91 Å, indicating the stable covalent bonding characteristics. For the ionic oxide Sc_2O_3 interface in Fig. 3(b), eight Ga atoms and four fourfold O atoms exist at the interface to satisfy the electron counting. These interfacial O species bond to one Sc atom on top and to three Ga atoms underneath, same as their bulk bonding characteristics. The interface roughness is 0.29 Å with an average Ga-O bond length of 2.08 Å, close to that in the bulk β-Ga_2O_3. The interfacial interaction barely affects the local bonding of the Al (Sc) atoms and N atoms. All these results indicate an energy-stable X_2O_3/GaN configuration.

The partial DOSs of the bulk layer GaN and oxide atoms that are sufficiently distanced away from the interface region in X_2O_3/GaN are presented in Fig. 4, where the valence band maximum (VBM) of the GaN bulk is aligned to zero for convenience. It is pictorial that the prudently built models have an insulating interface with no gap states in the bandgap, owing to the perfect satisfaction of the electron-counting rule. Both interfaces feature type-I band alignment with both the CBM and the VBM on the GaN side. This is consistent with the electron affinity as well as the experimental results. For power MOSFET applications, GaN's CBM should be assuredly lower than that of oxide dielectric; otherwise, electrons could not be effectively confined in the semiconductor side and lead to large leakage current.

When oxide and the semiconductor come in contact, discontinuous offsets (i.e., band offset) occur at both the valence band maximum (VBM) and the conduction band minimum (CBM).[12,13] The band offset value can be roughly determined using the partial DOS scheme for the band edge line-up in the interface supercell model.[31,32] The energy difference between their valence band maxima (i.e., VBO) is roughly observed to be 0.9 eV and 0.4 eV for Al_2O_3/GaN and Sc_2O_3/GaN in Fig. 4, respectively. Their counterpart CBOs are derived by using the calculated values of the band gaps of GaN (3.4 eV) and X_2O_3 (6.36 eV and 5.25 eV). In this work, we focus on another more accurate scheme to determine the band alignment using the core-level state,[22] for the assumption that the energy difference between the valence band maximum and the core-level state is maintained at a constant value even under different environments. We used the Ga-3*d* and O-2*s* core-level states in the bulk-like region, which are unaffected by the interface

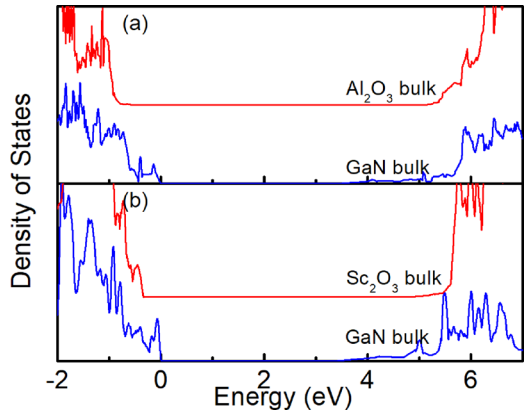

FIG. 4. Partial DOSs of the bulk layer GaN and oxide atoms that are far away from the interface region in the (a) Al_2O_3/GaN and (b) Sc_2O_3/GaN models. The valence band maximum (VBM) of the GaN bulk is aligned to 0 eV.

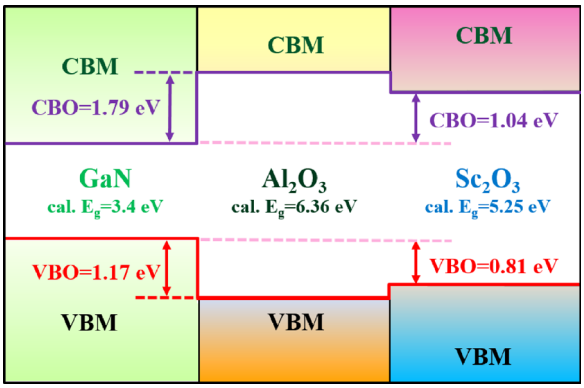

FIG. 5. Schematic band alignment diagram of Al_2O_3/GaN and Sc_2O_3/GaN interfaces using the core-level alignment. The valence band offset is determined using the core-level alignment method, which provides more accurate results. The CBO is defined as the difference between the calculated bandgap and the VBO values.

effect for reference, and derived the VBM of the individual side in the interface model with respect to this, and thus the VBO as the difference.

The schematic band alignment diagram of the X_2O_3/GaN interface using the core-level alignment is shown in Fig. 5. It is worth noting that the calculated bandgaps for Al_2O_3 and Sc_2O_3 are 6.36 eV and 5.25 eV, respectively, which are still 0.2 eV and 0.7 eV lower than the experimental data.[6,15] The results presented here can still be appreciated as the experimental bandgap value of GaN (E_g = 3.4 eV) is reproduced well. The calculated VBO is 1.17 eV for Al_2O_3/GaN and 0.81 eV for the Sc_2O_3/GaN interface, respectively. Taking advantage of the calculated oxide bandgap, the corresponding CBO is set to 1.79 eV and 1.04 eV, respectively.

It is meaningful to compare the calculated band alignment with the experimental values. All the experimental reported band offsets between Al_2O_3/GaN and Sc_2O_3/GaN are listed in Table I, with the calculated data (this work) for reference. It can be seen that the calculated

TABLE I. Band alignment comparison between our calculated X_2O_3/GaN interface values and the experimental reports. Note that the bandgap and BOs described in this work are all derived using "hybrid functional calculations."

E_g of Al_2O_3 (eV)	E_g of GaN (eV)	VBO (eV)	CBO (eV)	Data
6.36	3.4	1.17	1.79	This work
6.7	3.4	2.1	1.2	Ref. 6
6.5	3.4	1.8	1.3	Ref. 7
6.6	3.4	1.0	2.2	Ref. 8
…	…	0.7	…	Ref. 9
6.4	3.4	0.05	2.95	Ref. 14
E_g of Sc_2O_3 (eV)	E_g of GaN (eV)	VBO (eV)	CBO (eV)	Data
5.25	3.40	0.81	1.04	This work
6.0	3.44	0.42	2.14	Ref. 15
6.3	3.42	0.84	2.04	Ref. 16

VBOs all fall within the experiment range. At variance with the experimentally derived CBOs, the calculated CBOs are lower than several references. It is because the oxide bandgap is still underestimated (0.2 eV and 0.7 eV lower than those of the experimental data, respectively[6,15]). If taking advantage of the experimental bandgap (~6.6 eV for Al_2O_3 and ~6.0 for Sc_2O_3[6,15]) and our calculated VBOs, the newly derived CBO will be ~2.0 eV for the Al_2O_3 interface and ~1.8 for the Sc_2O_3 interface, which agrees better with the experimental conduction band offset values. Notably, the CBM on the GaN side is ~2.0 eV lower than that of X_2O_3 at both interfaces, well satisfying the 1 eV criterion for confining electrons on the semiconductor side.[12] In GaN-based power device applications, the gate electrode could suffer a large gate voltage to drive the power module. With the ~2.0 eV CBOs, the electrons can be effectively confined in the GaN side, further confirming that both Al_2O_3 and Sc_2O_3 are ideal dielectric materials for GaN-based MOSFET device applications.

In conclusion, the interfacial bonding, the electronic structures and the band offsets of Al_2O_3/GaN and Sc_2O_3/GaN interfaces were intensively investigated. By prudently modeling based on the electron counting rule, the insulating interface model with a small interfacial roughness and a clean bandgap was obtained. The valence band offset is derived to be ~1.2 and ~0.8 eV, respectively, coinciding well with the experimental results. The large conduction band offset (~2.0 eV) is sufficient for effectively confining the electrons in the GaN-based MOSFET device with Al_2O_3 or Sc_2O_3 as the gate dielectric.

The authors acknowledge funding from EPSRC Grant No. EP/P005152/1.

REFERENCES

[1]J. Y. Tsao, S. Chowdhury, M. A. Hollis, D. Jena, N. M. Johnson, K. A. Jones, R. J. Kaplar, S. Rajan, C. G. Van de Walle, E. Bellotti, C. L. Chua, R. Collazo, M. E. Coltrin, J. A. Cooper, K. R. Evans, S. Graham, T. A. Grotjohn, E. R. Heller, M. Higashiwaki, M. S. Islam, P. W. Juodawlkis, M. A. Khan, A. D. Koehler, J. H. Leach, U. K. Mishra, R. J. Nemanich, R. C. N. Pilawa-Podgurski, J. B. Shealy, Z. Sitar, M. J. Tadjer, A. F. Witulski, M. Wraback, and J. A. Simmons, Adv. Electron. Mater. **4**, 1600501 (2018).

[2]K. J. Chen, O. Häberlen, A. Lidow, C. L. Tsai, T. Ueda, Y. Uemoto, and Y. Wu, IEEE Trans. Electron Devices **64**, 779 (2017).

[3]R. Vetury, N. Q. Zhang, S. Keller, and U. K. Mishra, IEEE Trans. Electron Device **48**, 560 (2001).

[4]R. Mehandru, B. Luo, J. Kim, F. Ren, B. P. Gila, A. H. Onstine, C. R. Abernathy, S. J. Pearton, D. Gotthold, R. Birkhahn, B. Peres, R. Fitch, J. Gillespie, T. Jenkins, J. Sewell, D. Via, and A. Crespo, Appl. Phys. Lett. **82**, 2530 (2003).

[5]X. Wang, O. I. Saadat, B. Xi, X. Lou, R. J. Molnar, T. Palacios, and R. G. Gordon, Appl. Phys. Lett. **101**, 232109 (2012).

[6]J. Yang, B. S. Eller, and R. J. Nemanich, J. Appl. Phys. **116**, 123702 (2014).

[7]J. Yang, B. S. Eller, C. Zhu, C. England, and R. J. Nemanich, J. Appl. Phys. **112**, 53710 (2012).

[8]Y. Jia, J. S. Wallace, E. Echeverria, J. A. Gardella, and U. Singisetti, Phys. Status Solidi B **254**, 1600681 (2017).

[9]T. L. Duan, J. S. Pan, and D. S. Ang, Appl. Phys. Lett. **102**, 201604 (2013).

[10]S. Yang, Z. Tang, K. Wong, Y. Lin, C. Liu, Y. Lu, S. Huang, and K. J. Chen, IEEE Electron Device Lett. **34**, 1497 (2013).

[11]D. M. Zhernokletov, M. A. Negara, R. D. Long, S. Aloni, D. Nordlund, and P. C. McIntyre, ACS Appl. Mater. Interfaces **7**, 12774 (2015).

[12]J. Robertson, J. Vac. Sci. Technol. B **18**, 1785 (2000).

[13]Y. Guo, H. Li, S. J. Clark, and J. Robertson, J. Phys. Chem. C **123**, 5562 (2019).

[14]M. R. Coan, J. H. Woo, D. Johnson, I. R. Gatabi, and H. R. Harris, J. Appl. Phys. **112**, 24508 (2012).

[15]J. J. Chen, B. P. Gila, M. Hlad, A. Gerger, F. Ren, C. R. Abernathy, and S. J. Pearton, Appl. Phys. Lett. **88**, 142115 (2006).

[16]C. Liu, E. F. Chor, L. S. Tan, and Y. Dong, Phys. Status Solidi C **4**, 2330 (2007).

[17]M. D. Pashley, Phys. Rev. B **40**, 10481 (1989).

[18]L. Lin and J. Robertson, Appl. Phys. Lett. **98**, 82903 (2011).

[19]L. Lin, Y. Guo, R. Gillen, and J. Robertson, J. Appl. Phys. **113**, 134103 (2013).

[20]M. B. Pereira, E. M. Diniz, and S. Guerini, Adv. Condens. Matter Phys. **2015**, 1 (2015).

[21]K. Chokawa, E. Kojima, M. Araidai, and K. Shiraishi, Phys. Status Solidi B **255**, 1700323 (2018).

[22]E. A. Kraut, R. W. Grant, J. R. Waldrop, and S. P. Kowalczyk, Phys. Rev. Lett. **44**, 1620 (1980).

[23]S. J. Clark, M. D. Segall, C. J. Pickard, P. J. Hasnip, M. J. Probert, K. Refson, and M. C. Payne, Z. Kristallogr. **220**, 567 (2005).

[24]S. J. Clark and J. Robertson, Phys. Rev. B **82**, 85208 (2010).

[25]J. P. Perdew, K. Burke, and M. Ernzerhof, Phys. Rev. Lett. **77**, 3865 (1996).

[26]J. Heyd, G. E. Scuseria, and M. Ernzerhof, J. Chem. Phys. **124**, 219906 (2006).

[27]Z. Zhang, B. Li, Q. Qian, X. Tang, M. Hua, B. Huang, and K. J. Chen, IEEE Trans. Electron Devices **64**, 4036 (2017).

[28]Z. Zhang, Q. Qian, B. Li, and K. J. Chen, ACS Appl. Mater. Interfaces **10**, 17419 (2018).

[29]D. Liu, S. J. Clark, and J. Robertson, Appl. Phys. Lett. **96**, 32905 (2010).

[30]D. Liu and J. Robertson, Microelectron. Eng. **86**, 1668 (2009).

[31]L. Lin, K. Xiong, and J. Robertson, Appl. Phys. Lett. **97**, 242902 (2010).

[32]Z. Zhang, R. Cao, C. Wang, H. Li, H. Dong, W. Wang, F. Lu, Y. Cheng, X. Xie, H. Liu, K. Cho, R. Wallace, and W. Wang, ACS Appl. Mater. Interfaces **7**, 5141 (2015).